

Detection and Location of a Leak in a Gas-Transport Pipeline by a New Acoustic Method

YUKAWA, Hitoshi / MATSUKAWA, Shun / WATANABE, Kajiro / HIMMELBLAU, D.M. / 松川, 俊 / 渡辺, 嘉二郎 / 湯川, 等

(出版者 / Publisher)

法政大学工学部

(雑誌名 / Journal or Publication Title)

法政大学工学部研究集報 / 法政大学工学部研究集報

(巻 / Volume)

21

(開始ページ / Start Page)

129

(終了ページ / End Page)

157

(発行年 / Year)

1985-03

(URL)

<https://doi.org/10.15002/00004059>

Detection and Location of a Leak in a Gas-Transport Pipeline by a New Acoustic Method

Kajiro WATANABE*, Shun MATSUKAWA*, Hitoshi YUKAWA*,
D. M. HIMMELBLAU**

Abstract

We describe a new method for detecting and locating a leak in a gas transport pipeline lied between two pump stations by an indirect acoustic method. The basic concept is to treat the pipeline as an acoustic tube (similar to a wind instrument), and estimate the impulse response of the of the acoustic wave in the pipeline soley from the acoustic signal detected at two terminal sites in the pipeline. The test sigal introduced at the input site is only acoustic noise employed and pipeline operation would not be interrupted. If a leak occurs in the pipeline, the impulse response of the acoustic wave in the pipeline has a sharp pulse at a certain time that can be directly related to the site of the leak. Using the mathematical model of the pipeline acoustics ,i.e., the wave euation, we develop the tneoretical basis of how and why the leak can be detected and located. Experiments carried out in the laboratory under conditions comparable to realistic field conditions demonstrate the validity of the proposed detection method.

Scope

This work pertains to the diagnosis of faults (fault location and identifacation) in a physically widely dispersed pipeline system. In particular we treat the problem of leak detection and location in a gas-transport pipeline. Existing direct leak detection schemes that aim at locating the points at which leaks occur require inspection through the pipeline by people or require considerable expensive instrumentation, and in either case can be a slow and laborious. Existing indirect approaches aimed at deciding whether or not a leak exist, and/or localizing the leak site (s), cannot discover the leaking site (s) clearly and accurately.

We have developed a new method which (a) requires less effort and use more economical instrumentation than any of the existing direct methods, (b) does not require significant interruption of the pipeline operation, and (c) can locate the leak sites clearly and accurately. The basic idea underlying the proposed method is derived from the theory of wind instruments. We utilize the fact that the tone of a giant wind instrument (the pipeline)

* Department of Instrument and Control Engineering Cojjege of Engineering Hosei University
Koganei Tokyo 184 Japan

* * Chemical Engineering Departent The University of Texas at Austin Austin Texas 78712 U.S.A.

changes in the event of a leak, and we find this change by estimating the acoustic impulse response in the pipeline from acoustic signals detected at the two terminuses of the pipeline.

In addition to explaining the theoretical development that shows why and how the proposed method can detect and locate a leak in a pipeline, we present some experimental results collected under realistic operating conditions that validate the detection theory.

Conclusion and Significance

A new economic method of detecting and locating a leak in an operating gas-transport pipeline is presented. We conclude from the theoretical development of the leak detection method that the impulse responses of the acoustic wave in the pipeline estimated from acoustic signal measured at two end sites in the pipeline, should show conspicuous sharp positive or negative pulse at a certain time. The leak site can be determined from this pulse. Experiments carried out in our laboratory corresponding to realistic pipeline operations have demonstrated satisfactorily when the theoretical results are applied in practice, leaks can be located. The proposed method has the advantages that it is faster, requires less expensive and heavy instrumentation, and does not require cessation of pipeline operations as do many existing direct leak detection methods, and has the advantage relative to the existing indirect method that it can locate leak sites more clearly and correctly.

The method proposed here treated the problem to locate one leak occurred at a time in a single pipeline. In the case when more than one leak occurs at a time, the sites of leaks cannot be uniquely located but can be located as one of several sites. The number of presumable sites depends on the number of leaks. The theoretical development for the case of multiple leaks is somewhat complicated and we omitted to describe in this paper.

Introduction

A leak in a gas transport pipeline is always cause for concern as it may lead to a serious accident and damage may result. In order to prevent such accidents, online, quick and accurate detection and location of leaks is of major importance.

Two general approaches exist for leak detection, namely the direct approach, and the indirect approach. The direct approaches are simply those that confirm exact leak sites by inspection together with observation of secondary symptoms such as sound, smell, and visual detection of abnormal growth of vegetation due to the occurrence of leaks. Execution of the direct methods are usually carried out by line patrols following the pipeline right of ways or by local citizens' reports. Thus, most of the research work associated with the direct methods has been focused on developing sensitive and accurate detectors for the secondary symptoms. Decker (1978) reported on the effectiveness of a nitrous oxide tracer method which detects nitrous oxide that is outside of the pipeline by surveying from end to the

other and locates leak sites, the nitrous oxide gas fed at the pipeline inlet. Riemsijk and Bosselarr (1960) and Heim (1979) described a method to locate leak sites by detecting sonic and supersonic sound generated at a leaking site of a high pressure pipeline. Parker (1980) presented a detailed report describing how the supersonic sound is generated and propagated. Dallavalle *et. al.* (1977) described online leak detection (not location) in feedwater preheaters by monitoring the feedwater pressure noise. Cole (1979) lists patents granted for leak detection devices that use both direct and indirect measures in the period 1935-1976. Only one patent refers to microphones (more than one) to detect sonic waves. A method using an electric cable outside the pipeline whose electric properties are changed by leaked material (Sugaya; 1979) is also one of the direct methods. These direct methods essentially require inspections by human beings and always are finally applied to confirm the location of the leak site accurately. If the leak sites can be localized to a few areas in the pipeline, the methods are not too costly. Otherwise, they are slow and laborious, and cannot detect and locate leaks by an online, real time monitoring system.

The indirect approaches to leak detection are based on detecting leaks by measuring inlet-outlet (or spatially sparse) pipeline variables such as pressure and/or volumetric flow rate. The indirect methods originally were based on line balance methods which aimed at simply detecting the occurrence of leaks, not at locating leak sites. The line pack test that introduces high pressure gas or air to the pipeline and checks whether or not the pressure in the pipeline decreases with time, and the line balance method that investigates the steady state material balance of flow in and flow out are typical indirect methods commonly used in the field to find the existence of leaks (Sugaya; 1979). The steady state line balance methods, however, engender some uncertainty. Immediately after changes in the pipeline operating conditions, the transient pressure varies even if no leak occurs so that such methods can lead to errors in judgement. Many investigators have focused on how to compensate for this phenomena. Goldberg (1979) introduced the dynamic line balance model and reported that the method using his dynamic model demonstrated the ability to detect leaks under a wide range of flow conditions. Huber (1981) introduced a transient line balance model for the same purpose, and Lindsey and Vanelli (1981) also presented a similar model. Kreiss (1972) described a method which is based on detecting the change in the derivative of the volumetric flow rate.

Many recent investigations into indirect methods have focused on localizing the leak sites by spatially sparse online measurements from the pipeline. Schmidt and Lappus (1980) applied a Luenberger type observer to the model of a natural gas transport pipeline to find a leak site by estimating all of the state variables in the pipeline from the input and output measurements. Siebert and Isermann (1980) and Siebert (1981) improved and applied the hydraulic gradient method, a well known method to locate a leak site in hydraulic; a typ-

ical paper is that by Seiders (1979), to locate a leak in a gas pipeline. They improved the well known method by subtracting the reference mass flow measured under the normal operating condition from the current mass flow measured. They applied the cross-correlation method to suppress the effect of noises and to locate a small leak in a pipeline with compressible media like as gas. Huebler *et. al.* (1982) reported on the use of a single microphone placed inside a low pressure gas main to detect small leaks. A spectral analysis over the range of 0 to 100 kHz was used to locate the leaks from characterisitcs spectral pattern analysis. Watanabe (1980, 1982) presented a method to locate a leak site by estimating the acoustic propagation in the pipeline. These methods are quite interesting, but were mainly just theoretical studies to investigate the theoretical feasibility of leak detection, and were validated soley by computer simulations or by simplified experiments.

As for industrial leak detection systems, Phillips and Crider (1976) described a mini-computer system for leak detection that processed the measured data for system control using the steady state line balance method. Stewart (1980) on the other hand reported a leak detection system based on the dynamic line balance model.

The method presented in this paper is a new acoustic method which aims at locating a leak site in a single pipeline by the indirect approach. In this method we estimate the impulse response of the acoustic wave in the leaky pipeline. Knowledge of the impulse response of the acoustic wave in the pipeline locates the leak site. Below we first give a straightforward explanation how the impulse response of the acoustic wave can be used to identify the site of a leak, and then describe how the theory was verified by experiment.

Leak Detection and Location by an Acoustic Method

Assumptions

In explaining the principle of the proposed method of acoustic leak detection and location, the following simplifying assumptions are made; some of them may not necessarily be fullfilled in actual operation. By the term "test zone" of a pipeline, we mean the part of the pipeline, or the overall pipeline, to which the leak location method is applied.

- (1) The test zone of the pipeline has two constrictions, one at the input and one at the output ends.
- (2) The test zone of the pipeline is a sigle pipe with no branches.
- (3) Only one leak occurs in the test zone.
- (4) The test zone of the pipeline has uniform cross-sectional area for its entire length.
- (5) The pressure at the input end of the test zone includes random fluctuations whose spectral function is almost white.
- (6) Pressures inside and near the constrictions in the test zone can be measured by detectors or microphones having limited frequency bands.

- (7) Acoustic waves propagate in the pipeline without any attenuation and velocity of gas flow is negligible small in comparison with the sound velocity.

Assumption (1) is made to provide the boundary conditions that let the acoustic wave reflect at the input and output terminals of the test zone. Presumably the cross-sectional area of the constrictions is small relative to the cross-sectional area of the pipeline but the gas can flow through the two constrictions. Suppose the ratio (cross-sectional area of the constriction) / (cross-sectional area of the pipeline) = r , then the approximate acoustic reflection coefficient is estimated by $(1 - r) / (1 + r)$ and the coefficient r should be determined experimentally depending on the length and the cross-sectional area of the test zone. Further, there can be number of structures that the DC (constant) component of flow can pass through with less resistance but alternating (changing) flow component reflects. In the commercial service pipeline, we should design such the structure above. The constrictions or the equivalent structures should be placed in the part of pipeline that is in the pump station and are put into effect only when the leak location test is being carried out. Theoretically other type of boundary conditions might also make it possible to locate a leak, i. e., make the input and output of the test zone a chamber with wider cross-sectional area than that of the pipeline instead of using constrictions. In this case, only replacing the sound pressure that will be used in the following theoretical development or measurements into the sound volume velocity yields the same theoretical results and leak detection procedure. Making the chambers at the two ends of the test zone does not disturb any pipeline operation. But in this case we require the accurate measurements of volume velocity.

Assumption (2) is made to avoid the obvious feature that branches can be regarded as leaks.

Assumption (3) is made just to simplify the theoretical development. In practice, the probability that more than two leaks occur simultaneously in one test zone should be quite low except if the cause of leaks is earthquake.

Assumption (4) is also introduced to make the theoretical development easier. However, a single pipeline usually has only one cross-sectional area for long distances.

Assumption (5) is needed because at the input site of the test zone, we need a test signal which is noise with a broad band spectrum. If turbulent flow occurs near the input constriction, or if sound is generated by a compressor in the pump station, suitable noise is generated internally in the pipeline, and that noise can be used as the test signal. If such the noise does not exist, suitable noise has to be added at the inlet of the test zone. Variety of methods to generate and add the noises at the inlet of the test zone can be considered. As will be described in the section **Remarks**, choice of the long test zone requires the test noise with low and relatively narrow frequency band width but with high power.

Such the noise for example can be generated and added to the pipeline by using hydraulic servosystem that can respond to the random changes and or by pumping or changing gas flow by random way. Choice of the short test zone requires the test noise with high and broad frequency band width. Such the noise, for example, can be generated by an acoustic noise generator using a loud speaker and the noise can be added to the pipeline through the pipeline wall or by setting the loud speaker in a room beside the pipeline. The pressure of the room is almost same with that in the pipeline and the wall between the room and the pipeline is thin.

Assumption (6) means that the leak site is to be located solely by the pressure changes or acoustic waves in the pipeline measured at the input and output of the test zone. Thus we have to take into account the limitation of the frequency band of the detector in making the proposing leak detection method applicable in the realistic situations.

Assumption (7) means that the gas transported purely compressive and wall of the pipeline is thick and no acoustic energy pass through the wall. Further, velocity of gas flow in pipelines in commercial use is not high to keep the efficiency of transport high. It is known the velocity is in the range $10\text{m/sec} \sim 20\text{m/sec}$ except pipelines for special purposes.

Theory of Leak Detection and Location

Fig. 1 shows a sketch of a test zone which is a single pipe with no branches and with uniform cross-sectional area as required in Assumption (2) and (4), respectively and in which a leak may exist as required in Assumption (3). The input and output parts of the test zone contain constrictions as required in Assumption (1). The constrictions are realized by placing plates with a centered hole in the pipe. Shown as in Fig. 1, we let the input end of the test zone be origine of the distance (x) coordinate and the length of the test zone is L . We assume a leak with circle hole at ℓ that is a distance between the origine (input

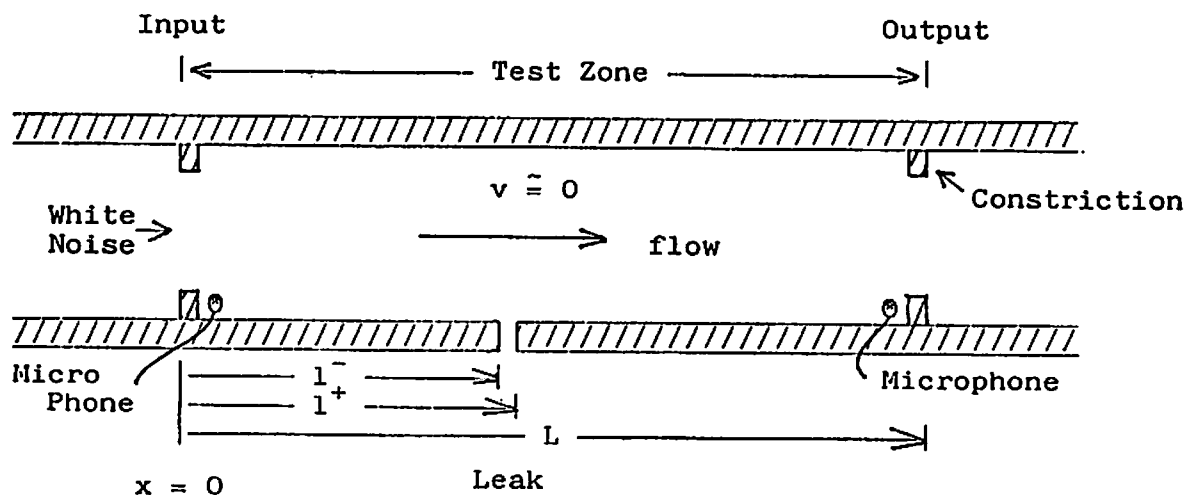


Fig. 1 A sketch of a pipeline test zone

end) and center of the circle leak hole. One end of the circle hole is at ℓ^- and the other end is at ℓ^+ as $\ell^- < \ell < \ell^+$ measured from the origine. Diameter of the leak ($\ell^+ - \ell^-$) is small relative to ℓ . White noise is added at the input end of the test zone as required in assumption (3) and the acoustic signals excited by the white noise are detected at the input site as $p_i(t)$ ($=p(0, t)$) and at the output site as $p_o(t)$ ($=p(L, t)$) by using microphones. We shall show how to locate the leak site ℓ from the measurements $p_i(t)$ and $p_o(t)$.

To make theoretical consideration more general, we first consider a case when gas flows in the pipeline with velocity v , even though we made the assumption that $v \cong 0$ in the later part of Assumption (7). From the former part of Assumption (7), the acoustic wave propagates without any attenuation in the pipeline, then the wave propagation can be described by a wave equation in the following form:

$$-\frac{1}{C_f} \frac{\partial f(x, t)}{\partial t} = \frac{\partial f(x, t)}{\partial x}, \quad f(L, t) + b(L, t) = 0 \quad (1-a)$$

$$-\frac{1}{C_b} \frac{\partial b(x, t)}{\partial t} = -\frac{\partial b(x, t)}{\partial x}, \quad \frac{\rho}{A} \{C_f f(0, t) - C_b b(0, t)\} = p_i(t) \quad (1b)$$

with

$$C_f = C_o + v \quad (1c)$$

$$C_b = C_o - v \quad (1d)$$

where

x is the distance from the input site of the test zone

t is the time

f is the sound volume velocity propagating forward

b is the sound volume velocity propagating backward

C_o is the velocity of sound which is determined by pressure and temperature. C_o should be calculated at first

v is the velocity of flow

C_f is the total velocity of sound propagating forward

C_b is the total velocity of sound propagating backward

A is the cross sectional area

ρ is the density of gas

The total sound volume velocity $u(x, t)$ and the sound pressure $p(x, t)$ is given by using the terms $f(x, t)$ and $b(x, t)$ as follows:

$$u(x, t) = f(x, t) + b(x, t) \quad (1e)$$

$$p(x, t) = \frac{\rho C_f}{A} f(x, t) - \frac{\rho C_b}{A} b(x, t) \quad (1f)$$

The sound pressure $p(x, t)$ and the sound volume velocity $u(x, t)$ are values that can be measured directly. When $v=0$, the wave equation is directly described by using the terms of $p(x, t)$ and $u(x, t)$.

First we divide the pipeline into three parts as follows :

$$(a) 0 \leq x < \ell^-, (b) \ell^- \leq x < \ell^+, (c) \ell^+ \leq x \leq L,$$

where $\ell^+ - \ell^-$ is the diameter of the circular hole of leak but has small value relative to the dipeline and the length of the test zone L , and we assume

$$\ell^+ \cong \ell^- \cong \ell \quad (1g)$$

The Fourier transform with respect to time of the wave equation (1a) and (1b) and substitution of the Fourier transformed $f(x, t)$ and $b(x, t)$ to eq. (1e) and (1f) for part (a) and (c) yields a well known 4-terminal network relation :

For part (a) :

$$\begin{bmatrix} P(\ell^-, i\omega) \\ U(\ell^-, i\omega) \end{bmatrix} = F(\ell^-) \begin{bmatrix} P(0, i\omega) \\ U(0, i\omega) \end{bmatrix} \quad (2a)$$

and for part (c) :

$$\begin{bmatrix} P(L, i\omega) \\ U(L, i\omega) \end{bmatrix} = F(L - \ell^+) \begin{bmatrix} P(\ell^+, i\omega) \\ U(\ell^+, i\omega) \end{bmatrix} \quad (2b)$$

where $P(x, i\omega)$ and $U(x, i\omega)$ are the Fourier transforms of $p(x, t)$ and $v(x, t)$, respectively, and the matrix function $F(z)$ is a transfer matrix defined by

$$F(z) = \exp(i\omega z/v') \begin{bmatrix} e_{11} & e_{12} \\ e_{21} & e_{22} \end{bmatrix} \quad (2c)$$

$$e_{11} = \cos\left(\frac{\omega z}{C'}\right) - i\left(\frac{v}{C_0}\right) \sin\left(\frac{\omega z}{C'}\right) \quad (2d)$$

$$e_{12} = -i\frac{\rho C_0}{A} \left(1 - \left(\frac{v}{C_0}\right)^2\right) \sin\left(\frac{\omega z}{C'}\right) \quad (2e)$$

$$e_{21} = -i\frac{\rho C_0}{A} \sin\frac{\omega z}{C'} \quad (2f)$$

$$e_{22} = \cos\frac{\omega z}{C_0} + i\left(\frac{C_0}{v}\right) \sin\frac{\omega z}{C'} \quad (2g)$$

where

$$i = \sqrt{-1}$$

$$v' = v \left\{ \left(\frac{C_0}{v}\right)^2 - 1 \right\} \quad (2h)$$

$$C' = C_0 \left\{ 1 - \left(\frac{v}{C_0}\right)^2 \right\} \quad (2i)$$

ω is the angular frequency

The transfer matrix for part (b), i. e., the leak site, of the pipeline is given by

$$\begin{bmatrix} P(\ell^+, i\omega) \\ U(\ell^+, i\omega) \end{bmatrix} = \begin{bmatrix} 1 & 0 \\ -1/Z_\ell & 1 \end{bmatrix} \begin{bmatrix} P(\ell^-, i\omega) \\ U(\ell^-, i\omega) \end{bmatrix} \quad (2j)$$

where Z_ℓ is the radiational acoustic impedance of the leak and is given by (Ohizumi, 1968)

$$Z = \frac{i\omega \frac{8\rho}{3\pi\sqrt{\pi d\tilde{k}}}}{1 + i\omega \left(\frac{3v/d\pi}{16C_o}\right)} \quad (2k)$$

where

d is the cross sectional area of the leak (assuming the leak is circle)

\tilde{k} is the compensating coefficient.

If one is interested in the frequencies in the following range

$$0 \leq \omega \ll \frac{16C_o}{3\sqrt{\pi d}} \quad (2l)$$

(such as when the diameter of the leak is 5 mm so that $\omega = 2.33 \times 10^6 \text{ rad/sec} = 371 \text{ kHz}$), the impedance can be approximated by

$$Z_\ell \cong i\omega \frac{8\rho}{3\pi\sqrt{\pi d\tilde{k}}} \quad (2m)$$

Elimination of $P(\ell^-, i\omega)$, $U(\ell^-, i\omega)$, $P(\ell^+, i\omega)$ and $U(\ell^+, i\omega)$ from eqs. (2a), (2b) and (2j) yields an effective transfer matrix

$$\begin{bmatrix} P(L, i\omega) \\ U(L, i\omega) \end{bmatrix} = F(L-\ell^+) \begin{bmatrix} 1 & 0 \\ -1/Z_\ell & 1 \end{bmatrix} F(\ell^-) \begin{bmatrix} P(0, i\omega) \\ U(0, i\omega) \end{bmatrix} \quad (3a)$$

or

$$\begin{bmatrix} P(L, i\omega) \\ U(L, i\omega) \end{bmatrix} = \begin{bmatrix} f_{11} & f_{12} \\ f_{21} & f_{22} \end{bmatrix} \begin{bmatrix} P(0, i\omega) \\ U(0, i\omega) \end{bmatrix} \quad (3b)$$

Based on assumption (1), the pipeline being constricted at $x=L$, i.e., from the boundary condition in eq. (1a) and (1e) we can let

$$U(L, i\omega) \cong 0 \quad (3c)$$

Thus, from eq. (3b) we have a transfer function that characterizes the signal transformation from $P(L, i\omega)$ to $P(0, i\omega)$ in the frequency domain as follows:

$$\begin{aligned} \frac{P(0, i\omega)}{P(L, i\omega)} &= f_{22} = G(i\omega) \\ &= \exp(i\omega L/v') \left[\left\{ 1 + \frac{\rho v}{2Z_\ell A} \left(1 - \left(\frac{v}{C_o} \right)^2 \right) \right\} \cos \frac{\omega L}{C'} \right. \\ &\quad + i \left\{ \frac{v}{C_o} + \frac{\rho v}{2Z_\ell A} \left(1 - \left(\frac{v}{C_o} \right)^2 \right) \right\} \sin \frac{\omega L}{C'} \\ &\quad + i \frac{\rho C_o}{2Z_\ell A} \left(1 - \left(\frac{v}{C_o} \right)^2 \right) \sin \frac{\omega(2\ell-L)}{C'} \\ &\quad \left. - \frac{\rho v}{2Z_\ell A} \left(1 - \left(\frac{v}{C_o} \right)^2 \right) \cos \frac{\omega(2\ell-L)}{C'} \right] \quad (4a) \end{aligned}$$

From Assumption (7), if $v \cong 0$ and if the radiational impedance Z_ℓ can be approximated by eq. (2m), the transfer function (4a) becomes

$$G(i\omega) = \cos \frac{\omega L}{C_o} + \frac{3\pi\sqrt{\pi d k C_o}}{16A\omega} \left(\sin \frac{\omega L}{C_o} - \sin \frac{\omega(2\ell-L)}{C_o} \right) \quad (4b)$$

or

$$G(i\omega) = \cos \frac{\omega L}{C_o} + \frac{K}{\omega} \sin \frac{\omega L}{C_o} + \frac{K}{\omega} \sin \frac{\omega(2\ell-L)}{C_o} \quad (4c)$$

where

$$K = \frac{3\pi\sqrt{\pi d k C_o}}{16A} \quad (4d)$$

Transfer function (4c) is a real function including periodic and dumped periodic functions of frequency ω . Fig. 2 shows the frequency responses of each three terms in eq. (4c) and the total of the three above. This transfer function is the basic relation to locate the leak site by the method proposed here. The last term of the right hand side of eq. (4c) or the third term in Fig. 2 includes the information of the leak site ℓ which can be determined by the longest period $C_o/|2\ell-L|$ and the sign of the component with longest period in the estimated transfer function. The estimated transfer function that corresponds to eq. (4c) is obtained by the Fourier transform of the measurements $P_o(t)$ and $P_i(t)$ and by dividing the Fourier transformed $p_i(t)$ by the Fourier transformed $p_o(t)$ as the left hand side of eq. (4a). However, direct estimation of the period and sign of the last term of eq. (4c) from the estimated transfer function may lead to confusion and difficulty because:

- (1) It is difficult to pick up the information of the last term in eq. (4c) from the summation of the three terms. (See for example Fig. 2, it is hard to pick up the third term from the total frequency response.)
- (2) The transfer function $G(i\omega)$ estimated from the real measurements $p_i(t)$ and $p_o(t)$ may be noise corrupted.

Thus in order to enhance and to make it easy to pick up the accurate period and sign of the term with the longest period from the estimated $G(i\omega)$, we just apply the Fourier analysis by which the period and sign can be straightforwardly obtained from the noisy transfer function. Because eq. (4c) is real spectral function, we apply the inverse Fourier cosine transform instead of the Fourier transform. In fact, the inverse Fourier cosine transform plays the same role with the Fourier cosine transform itself. To make the discussion fit to the assumption (6), we obtain the inverse Fourier transform for the limited frequency band width $\omega_i \leq \omega \leq \omega_h$. The inverse Fourier transform becomes

$$\begin{aligned} g(t) &= \frac{2}{\pi} \int_{\omega_i}^{\omega_h} G(i\omega) \cos \omega t d\omega \\ &= \frac{2}{\pi} \int_{\omega_i}^{\omega_h} \cos \frac{\omega L}{C_o} \cos \omega t d\omega + \frac{2K}{\pi} \int_{\omega_i}^{\omega_h} \frac{\sin \frac{\omega L}{C_o} \cos \omega t}{\omega} d\omega + \frac{2K}{\pi} \int_{\omega_i}^{\omega_h} \frac{\sin \frac{\omega(\ell-L)}{C_o} \cos \omega t}{\omega} d\omega \\ &= g_1(t) + g_2(t) + g_3(t) \end{aligned} \quad (4e)$$

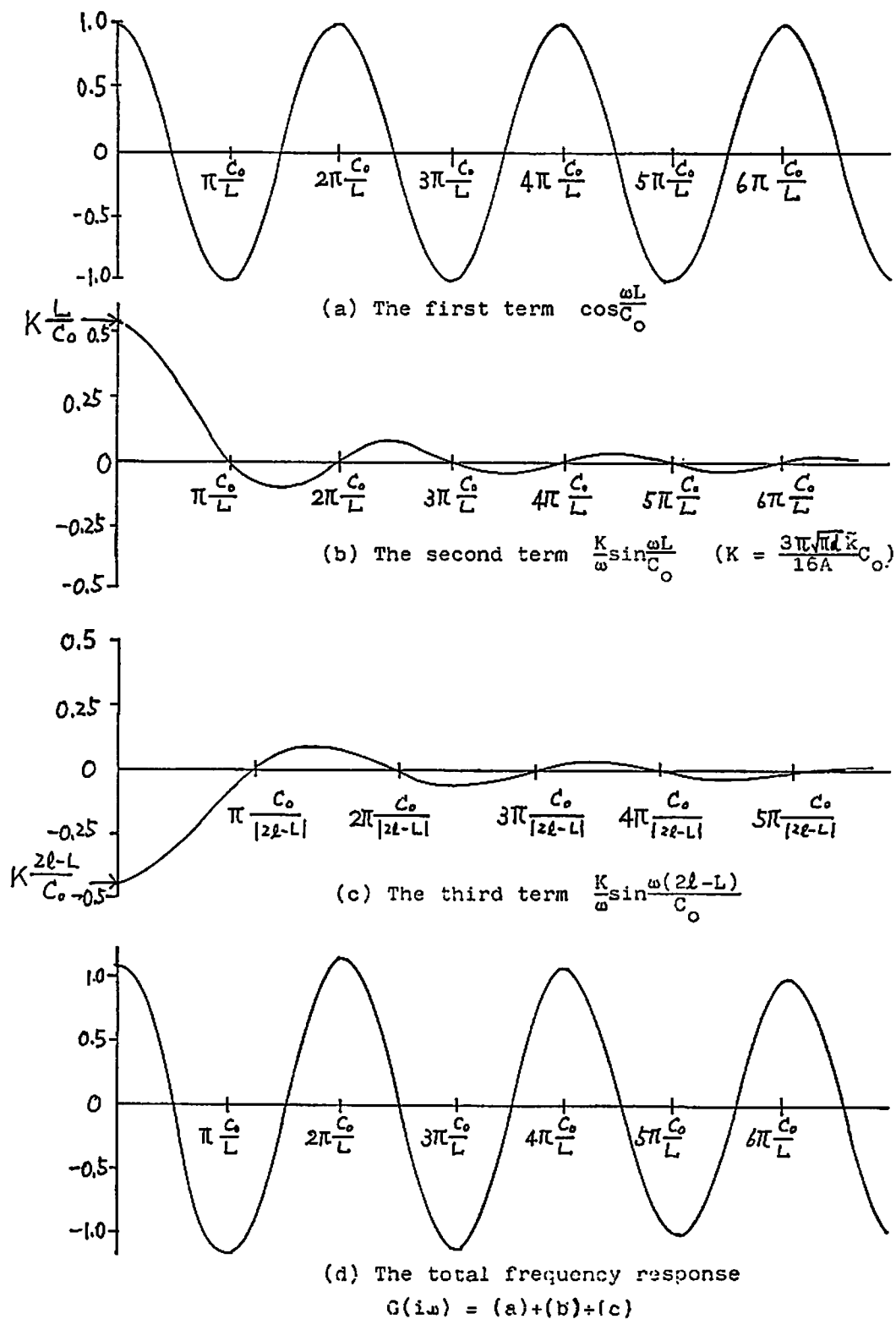


Fig. 2 Frequency response of each term in eq. (4c)

where

$$g_1(t) = \frac{1}{\pi} \left[\frac{1}{L/C_0 + t} \left\{ \sin\left(\frac{L}{C_0} + t\right)\omega_h - \sin\left(\frac{L}{C_0} + t\right)\omega_l \right\} + \frac{1}{L/C_0 - t} \left\{ \sin\left(\frac{L}{C_0} - t\right)\omega_h - \sin\left(\frac{L}{C_0} - t\right)\omega_l \right\} \right]$$

$$g_2(t) = \frac{2K}{\pi} [\text{Si}\{\omega_h(t + \frac{L}{C_o})\} - \text{Si}\{\omega_h(t - \frac{L}{C_o})\} - \text{Si}\{\omega_l(t + \frac{L}{C_o})\} + \text{Si}\{\omega_l(t - \frac{L}{C_o})\}] \quad (4f)$$

$$g_3(t) = \frac{2K}{\pi} [\text{Si}\{\omega_h(t + \frac{2\ell - L}{C_o})\} - \text{Si}\{\omega_h(t - \frac{2\ell - L}{C_o})\} - \text{Si}\{\omega_l(t + \frac{2\ell - L}{C_o})\} + \text{Si}\{\omega_l(t - \frac{2\ell - L}{C_o})\}]$$

with

$$\text{Si}(a(t+c)) - \text{Si}(a(t-c)) = \int_c^a \frac{\sin b\omega \cos \omega t}{\omega} d\omega \quad (4g)$$

The first term $g_1(t)$ and the second term $g_2(t)$ show a sharp positive pulse at time $t_L = L/C_o$ that corresponds to the time it takes sound to travel the length of the test zone. The third term $g_3(t)$ shows a sharp positive or negative pulse at time $t_\ell = |2\ell - L|/C_o$. The pulses by $g_1(t)$ and $g_2(t)$ and that by $g_3(t)$ become sharper as $\omega_h - \omega_l$ is increased.

If $\ell \leq L/2$, the last term in eq. (4c) by which the leak site is determined, can be re-written as

$$\frac{K}{\omega} \sin \frac{\omega(2\ell - L)}{C_o} = -\frac{K}{\omega} \sin \frac{\omega(L - 2\ell)}{C_o} \quad (4h)$$

Thus the inverse Fourier cosine transform has a negative sharp pulse at time

$$t_\ell = \frac{L - 2\ell}{C_o} \quad (4i)$$

which leads to

$$\ell = \frac{1}{2}(L - C_o t_\ell) \quad (5a)$$

Then if $g(t)$, the inverse Fourier cosine transform has a negative sharp pulse at $t = t_\ell (\neq t_L)$, the leak site can be determined by eq. (5a). Similarly, if $g(t)$ has the positive sharp pulse at $t = t_\ell$, the leak site must be $\ell \geq L/2$ and the site can be determined by

$$\ell = \frac{1}{2}(L + C_o t_\ell) \quad (5b)$$

Fig. 3 shows a sketch to demonstrate the relation between the leak site and how the pulse occurs in $g(t)$. Note shown as in Fig. 3, one or two pulse(s) occurs in the time function $g(t)$ in the period $[0, t_L]$. One of them must always occur at $t_L = L/C_o$, and must be positive, and if there is a leak, the second pulse must be occur in the period $[0, t_L]$.

Procedure to Calculate the Frequency and Impulse Responses

The frequency response $G(m)$ ($=G(i2\pi m/N\tau)$) corresponding to eq. (4c) and the impulse response $g(k)$ ($=g(k\tau)$) corresponding to eq. (4e) were obtained by applying the Fourier analysis. Because the data $p_i(t)$ and $p_o(t)$ are measured discretely, the discrete Fourier transform (DFT) and the inverse discrete Fourier transform (IDFT) are used instead of the Fourier and inverse Fourier transform, respectively. The operations DFT and IDFT are performed very quickly by using the fast Fourier transform (FFT) algorithm. The calculation procedure using the DFT and IDFT operations is as follows:

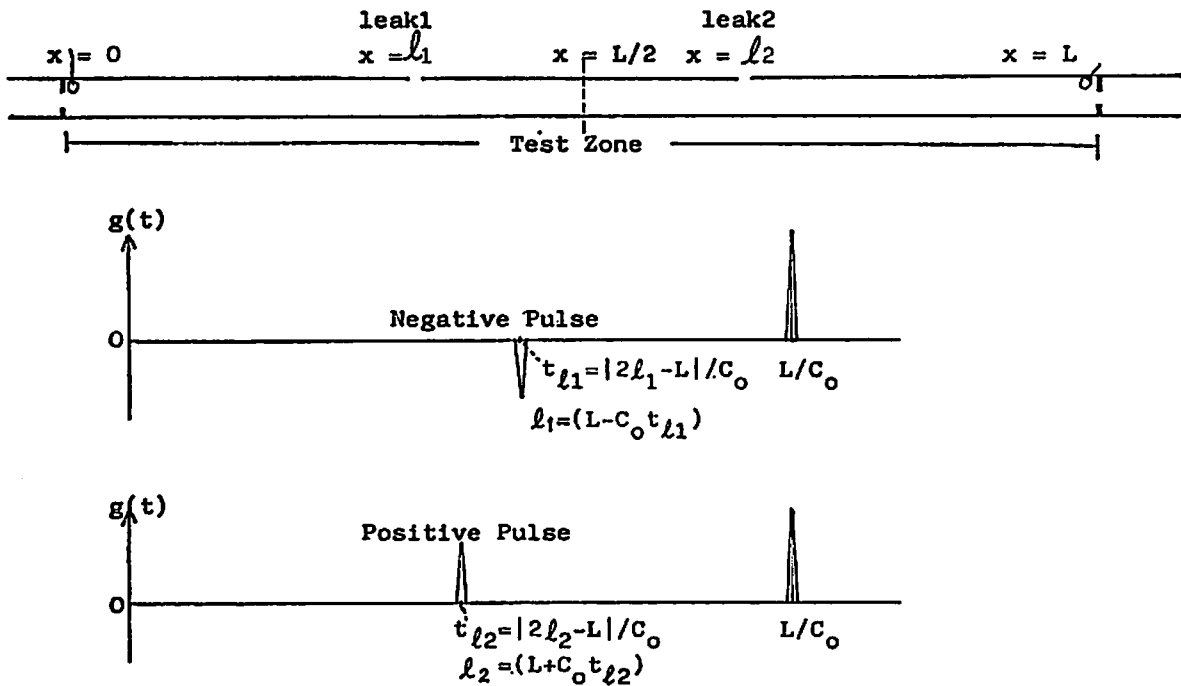


Fig. 3 Relation between leak site and the impulse response

(i) Define

τ is the sampling interval in the discrete measurements of $p_i(t)$ and $p_o(t)$

k is the discrete time with sampling interval τ

m is the discrete frequency with step $i\Delta\omega = i(2\pi/N\tau)$

N is the number of the data $p_i(k)$ or $p_o(k)$

$p_i(k)$ and $p_o(k)$ are the input and output data measured First calculate

$$\tilde{G}(m) = \frac{\text{DFT}(p_i(k))}{\text{DFT}(p_o(k))} \quad (6a)$$

(ii) Then obtain

$$\begin{aligned} \bar{G}(m) = & \frac{1}{429} [-36(\tilde{G}(m-5) + \tilde{G}(m+5)) + 9(\tilde{G}(m-4) + \tilde{G}(m+4)) + 44(\tilde{G}(m-3) \\ & + \tilde{G}(m+3)) + 69((\tilde{G}(m-2) + \tilde{G}(m+2)) + 84(\tilde{G}(m-1) + \tilde{G}(m+1)) + 89\tilde{G}(m)] \end{aligned} \quad (6b)$$

and $\hat{G}(m)$

$$\hat{G}(m) = \begin{cases} \bar{G}(m) & \text{if } |\bar{G}(m)| > 2|\tilde{G}(m)| \\ \text{otherwise } \tilde{G}(m) \end{cases} \quad (6c)$$

The procedure outlined in (ii) avoids ill effects due to division by $\text{DFT}(p_o(k))$ in eq. (6a). Note that from eq. (4c), $G(i\omega)$ is given by summation of $\cos(\omega L/C_o)$, $(K/\omega)\sin(\omega L/C_o)$ and $(K/\omega)\sin(\omega(2\ell-L)/C_o)$ then $G(i\omega)$ must be bounded above and below by a certain value. However $\tilde{G}(m)$ in eq. (6a) can have big value in the form of a pulse at some m due to division by zero in the calculation of (6a). The operation (6c) is designed to suppress such big pulses.

(iii) Apply a window operation

From eq. (4c), we know that $G(i\omega)$ is a continuous smooth function. Thus, a window which substantially suppresses small fluctuation, in $\hat{G}(m)$ can be effectively applied. We applied a window eq. (6b) which is a spectrum window that makes $\hat{G}(m)$ smooth by cutting off the fluctuations in $\hat{G}(m)$ in the sense of least squares error for the period $[(m-5), (m+5)]$ to eq. (6c) to get a smoother frequency response.

$$G(m) = \frac{1}{429} [-36(\hat{G}(m-5) + \hat{G}(m+5)) + 9(\hat{G}(m-4) + \hat{G}(m+4)) + 44(\hat{G}(m-3) + \hat{G}(m+3)) + 69(\hat{G}(m-2) + \hat{G}(m+2)) + 84(\hat{G}(m+1) + \hat{G}(m+1)) + 89\hat{G}(m)] \quad (6d)$$

(iv) Calculate $g(k)$

Recall from eq. (4c) that $G(i\omega)$ is real. Thus, the impulse response $g(k)$ can be obtained by applying the inverse Fourier cosine transform. Let $Re\{G(m)\}$ be real part of a complex number $G(m)$, then the inverse Fourier cosine transform for the discrete data can be calculated by using the IDFT as follow :

$$g(k) = \text{IDFT}[Re\{G(m)\} + i0] \quad (6e)$$

Remarks

We have described assumptions, theoretical basis and procedure (algorithm) of the acoustic method proposed in this paper. We will provide here some remarks about limitations of the proposed method and guide lines in selections of frequency band width of the noise generator and the acoustic detectors, sampling interval in the measurements and number of data points.

Effect of Length of the Test Zone and Frequency Band Width of the Detectors and Noise Generator

The shortest length of the test zone is determined by the sampling interval in the discrete measurements of $p_i(t)$ and $p_o(t)$. From equations (5) that relate the (leak) site and time (when pulse occurs), discretization of continuous data with the sampling interval leads to discretization of the pipeline with respect to length. The unit length corresponding to is given by

$$\Delta x = \frac{\tau C_o}{2} \quad (\tau = \frac{2\Delta x}{C_o}) \quad (7a)$$

The length Δx is the shortest length permissible and is the minimum resolution of identifiability of the leak site.

The longest length of the test zone permissible can be determined by how accurately one can identify the last term in eq. (4c). Fig. 2 showed the frequency responses of each term in eq. (4c) and eq. (4c) itself. From eq. (4c), the magnitude of the last term of eq.

(4c) is obtained as follow :

$$\begin{aligned} \left(\text{Magnitude of the term } \frac{K}{\omega} \sin \frac{\omega(2\ell-L)}{C_o}\right) &= \frac{K}{\omega} \sin \frac{\omega(2\ell-L)}{C_o} \Big|_{\omega=0} \\ &= K \frac{(2\ell-L)}{C_o} = \left(K \frac{(2\ell/L)-1}{C_o}\right) L \end{aligned} \quad (7b)$$

Further the frequency range that satisfy

$$0.05 \left| K \frac{2\ell-L}{C_o} \right| \leq \left| \frac{K}{\omega} \sin \frac{\omega(2\ell-L)}{C_o} \right|$$

i. e., the frequency range in which magnitude of spectrum of the last term in eq. (4c) is greater than 5 % of $(K(2\ell-L)/C_o)$ is obtained as

$$0 \leq \omega \leq \frac{5.67\pi C_o}{|2\ell-L|} = \frac{5.67\pi C_o}{|(2\ell/L)-1|} \frac{1}{L} \quad (7c)$$

From eq. (7b) and eq. (7c), we can observe :

- (1) As $\ell \rightarrow (L/2)$, the magnitude of $(K(2\ell-L)/C_o) \rightarrow 0$ and the upper bound of the frequency range $(5.67\pi C_o/(2\ell-L)) \rightarrow \infty$. This means if a leak occurs near the midpoint of the test zone, identification of the transfer function of the last term in eq. (4c) becomes difficult. Conversely, identification of a leak which is in the area of $\ell \rightarrow 0$ or $\ell \rightarrow L$ is easy.
- (2) For a fixed $\ell/L (\neq 0.5)$, as the length L of the test zone increases, the magnitude $(K(\ell/L-1)/C_o)L$ increases and the upper bound $((5.67\pi C_o)/(2\ell/|L-1|))(1/L)$ of the frequency range decreases. This means that the longer choice of the test zone provides a situation that the transfer function of the last term in eq. (4c) must and/or can be identified in a narrow range of frequency with relatively high power spectrum data calculated by equations (6). This fact indicates that the range of spectrum of the test noise and frequency band width of acoustic detectors can be narrow.

From eq. (7a), (7b) and (7c) and the observation (1) and (2) above, we can derive guidelines how to select the frequency bandwidth of the noise generator and acoustic detectors, sampling interval, and number of data points N . In the following discussion we assume that $0 \leq \ell/L \leq 0.45$ or $0.55 \leq \ell/L \leq 1$. By letting $\ell/L=0.45$ or $\ell/L=0.55$, the magnitude given by eq. (7b) and the upper bound of frequency range given by (7c) become as follows :

$$K \left(\frac{2\ell-L}{C_o} \right) = \frac{K}{10C_o} L, \frac{5.67\pi C_o}{|(2\ell/L)-1|} \frac{1}{L} = \frac{56.7\pi C_o}{L} \quad (7d)$$

Thus, guidelines are :

- (1) Frequency responses of the noise generator and the acoustic detector should be flat for the following frequency range :

$$0 \leq \omega \leq \omega_m, \omega_m \geq \frac{56.7\pi C_o}{L} \quad (7e)$$

- (2) From the Shannon's theorem, the sampling interval τ is determined by

$$\tau = \frac{\pi}{\omega_m} \quad (7f)$$

and from eq. (7a), the shortest length of the pipeline or minimum resolution of identifiability of the leak site becomes

$$\Delta x = \frac{\pi C_o}{2\omega_m} \quad (7g)$$

(3) If $\ell/L=0$ or $\ell/L=1$, the period of the last term of eq. (4c) becomes $2\pi C_o/L$. To calculate DFT, the sampling width $\Delta\omega$ of frequency should be much greater than the period, i. e.,

$$2\pi \frac{C_o}{L} \gg \Delta\omega = \frac{2\pi}{N\tau} \quad (7h)$$

which leads to

$$N \gg \frac{1}{\tau C_o} = \frac{\omega_m L}{\pi C_o} \quad (7i)$$

From eq. (7h), choice of the number of data points N larger yields the smaller width of frequency sampling $\Delta\omega$ by which frequency response calculated includes the desired information in the significant frequency range. Thus, longer time record yields the more accurate leak location result.

Use of Process Noise as the Test Signal

The process noise such as compressor noise, turbulent noise and valve noise can be used as the test signal, if the noise is generated near the input end of the test zone and if the spectrum of noise has high power in the frequency range

$$0 \leq \omega \leq \omega_m \quad (7j)$$

where ω_m is defined in eq. (7e).

In this case, the procedure to calculate the frequency and impulse response is essentially the same as that given by eq. (6a) to eq. (6e). But before calculating eq. (6a), we need to check whether or not the results of the DFT of $p_i(k)$ and $p_o(k)$ have significant power spectrum in the frequency range eq. (7j).

A sine wave generator can be used instead of using the noise generator or the process noise to estimate the transfer function eq. (4c). Use of the sine wave signal may serve as a better estimate in the noisy pipeline. However, estimation of gain as well as phase of the transfer function (4c) requires time-consuming and tedious work. Besides, the sine wave generator with resolution of $\Delta\omega$ (if L is long) is expensive.

Effect of Cross-Sectional Area of the Pipeline

From eq. (4c), the magnitude of the last term decreases in inverse proportion to the cross-sectional area of the pipeline. This means that the magnitude of the spectral function $G(i\omega)$ used to locate the leak site decreases in proportion to the increase of the cross-sectional area A of the pipeline for a leak with the same cross-sectional area.

Experiments

Experimental System

Experiments were carried out using the laboratory pipeline shown in Fig.4 (a). The pipeline was constructed by using 19 iron pipes of about 2.75 m length and 18 PVC junctions each of about 0.4 m length. The diameter of the inside of pipe was 22.1 mm (the cross sectional area $A=3.83 \times 10^{-4} m^2$). The length L of the test zone was selected to be 58.8 m. The input and output of the test zone were constricted by two plates each with a centered hole 10 mm in diameter. Experiments were carried out when temperature was 291 K (19°C), i. e., the sound velocity was $C_0=344$ m/sec for three cases (1) a leak was cut at $\ell=2.18$ m, (2) the leak (1) was closed and a leak was cut at $\ell=17.73$ m, and (3) the leaks (1) and (2) were closed and a leak was cut at 39.76 m with the same cross-sectional area $d=1.96 \times 10^{-5} m^2$. The gas did not flow in the pipe during the test.

Noise generated by a 17 bits M-sequence generator with a clock time of 1 msec, ampli-

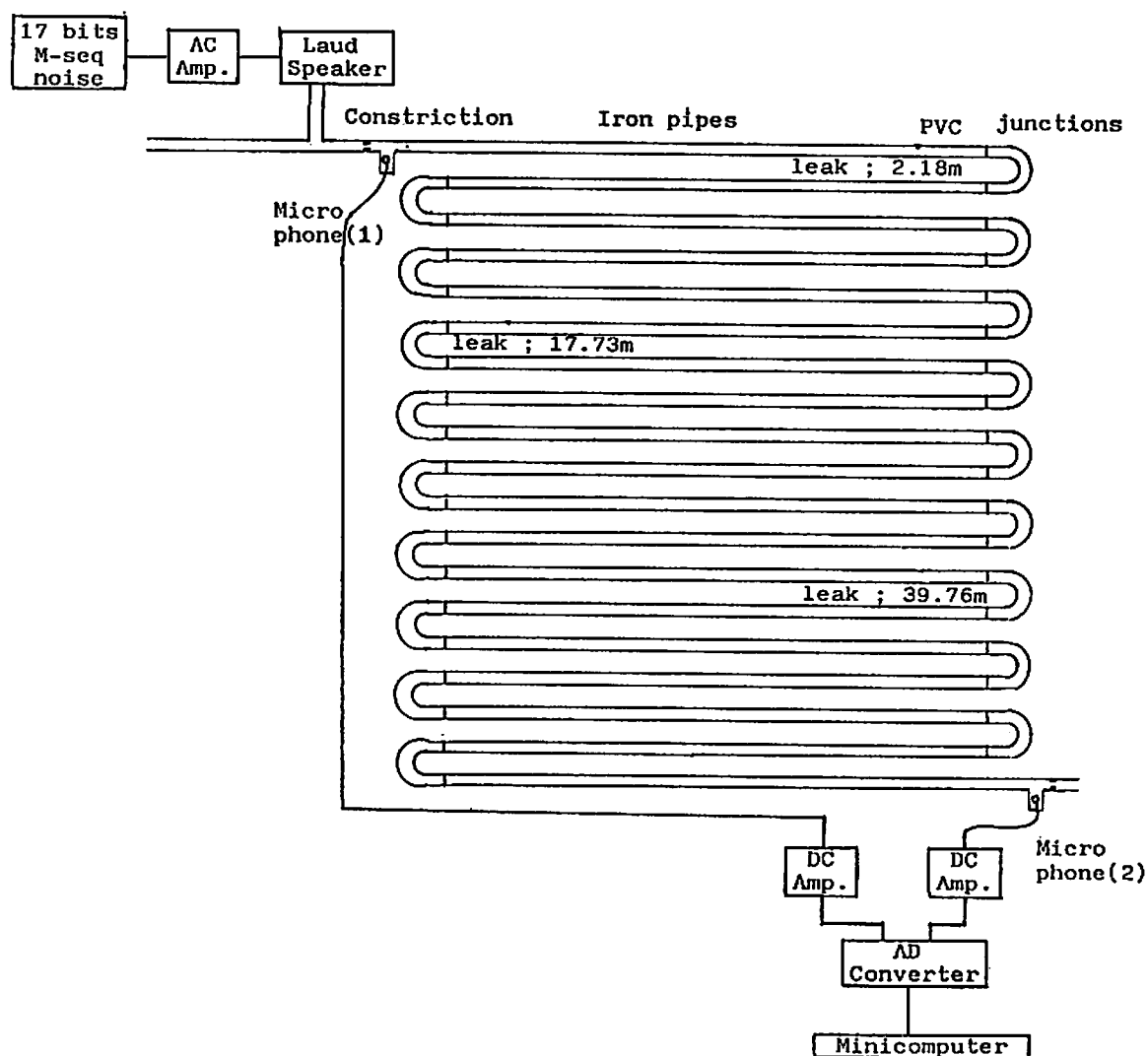


Fig. 4 (a) Experimental System

fied by an AC amplifier and actuated by a loud speaker with the frequency response shown as in Fig. 4 (b), was added at the input site of the test zone of the pipeline. Figures 4 (b), 4(c) and 4(d) indicate the range of frequency in measuring $p_i(t)$ and $p_o(t)$ is determined by that of the loud speaker which has the narrowest band width among three frequency responses, Fig. 4 (b), Fig. 4 (c) and Fig. 4 (d). Thus, from Fig. 4 (b), the frequency band corresponding to $\omega_i \leq \omega \leq \omega_h$ for integration of eq. (4e) becomes

$$\omega_i = 690 \text{ rad/sec (110 Hz)} \leq \omega \leq \omega_h = 2137 \text{ rad/sec (340 Hz)}$$

The input signal $p_i(t)$ detected by microphone (1) (which had the frequency response shown in Fig. 4 (c)) and the output signal $p_o(t)$ detected by microphone (2) (which had the fre-

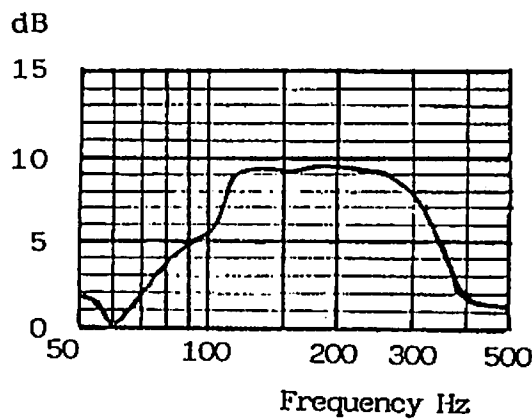


Fig. 4 (b) Frequency response of the loud speaker used as a noise source

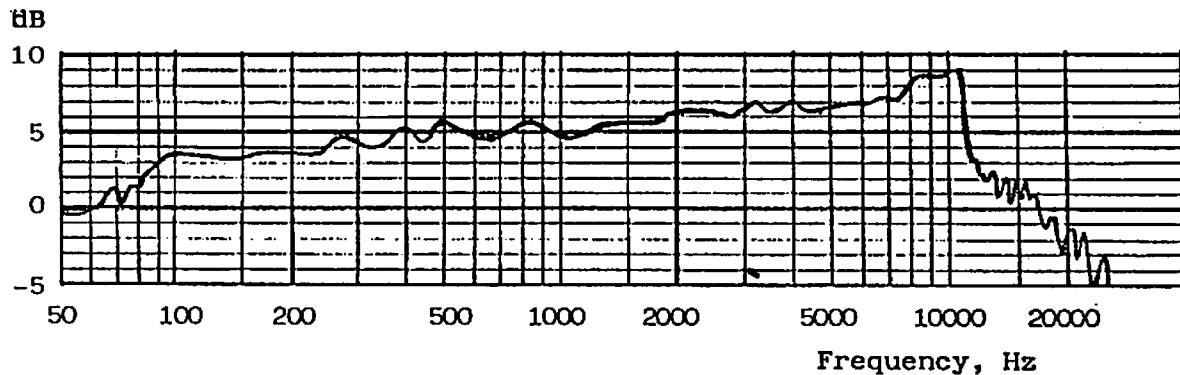


Fig. 4 (c) Frequency response of microphone (2)

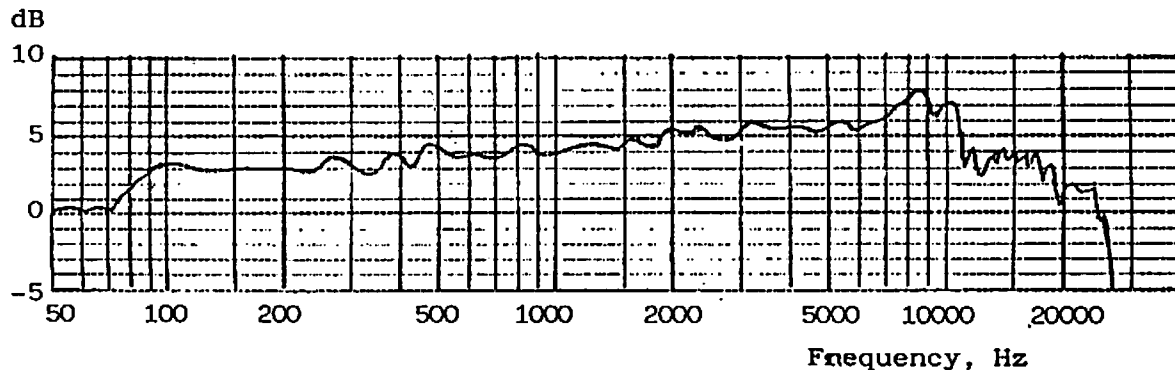


Fig. 4 (d) Frequency response of microphone (1)

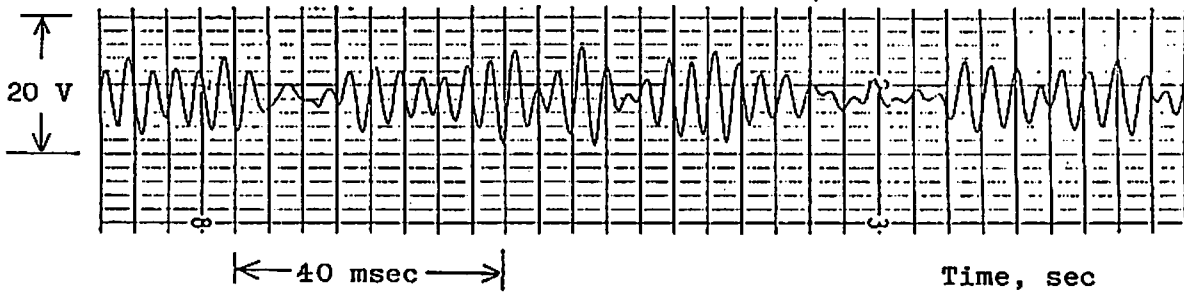


Fig. 4 (e) Measurement $P_i(t)$ by microphone (1) for a leak at $\ell = 2.18\text{m}$

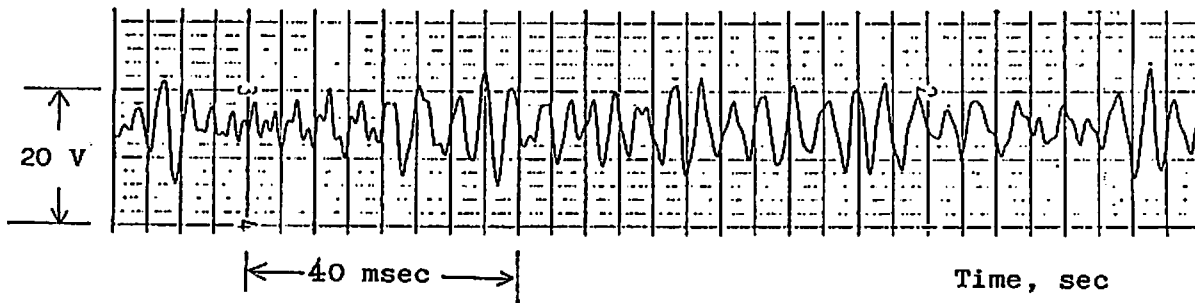


Fig. 4 (f) Measurement $P_o(t)$ by microphone (2) for a leak at $\ell = 2.18\text{m}$

frequency response shown as in Fig. 4 (d)) are shown in Fig. 4 (e) and Fig. 4 (f), respectively for a leak at $\ell = 2.18\text{m}$ measured from the input site.

The signals $p_i(t)$ and $p_o(t)$ were discretized with a sampling interval of $\tau = 1.470\text{msec}$ by a 12 bits AD converter for which the hold over frequency was 2137rad/sec , a value that is almost equal to ω_h of the loud speaker. The number N of the discrete data point equaled 2048.

Supposing that $\omega_h = \omega_m (= 2137\text{rad/sec})$ defined in eq. (7e), the above choice of τ and N satisfies the conditions (7f), (7g) and (7j) as follows:

$$\omega_m = 2137\text{rad/sec} > (56.7 \pi C_o / L) = 1042\text{rad/sec}$$

$$\tau = (\pi / \omega_m) = 1.470\text{msec}$$

$$N = 2048 \gg (\omega_m L / \pi C_o) = 116.3$$

Further, the minimum resolution of identifiability of the leak site becomes

$$\Delta x = (\pi C_o / 2\omega_m) = 0.253\text{m}$$

The DC amplifiers used to amplify the signals $p_i(t)$ and $p_o(t)$ were adjusted so that the AD converter worked with full bits.

Simulation Results

First, we will describe some results of simulations and then compare them with the experimental results. The impulse response function $g(t)$ in eq. (4e) was calculated for the same conditions as used in the experimental system, i. e., $L = 58.8\text{m}$, $C_o = 344\text{m/sec}$, $A = 3.83 \times 10^{-4}\text{m}^2$, $d = 1.96 \times 10^{-5}\text{m}^2$, $\omega_i = 960\text{rad/sec}$, $\omega_h = 2130\text{rad/sec}$, $\tilde{k} = 1$, for each of the three leak sites $\ell = 2.18\text{m}$, $\ell = 17.73\text{m}$, and $\ell = 39.76\text{m}$, respectively.

Based on the theory for leak detection and location, for the case in which no leak

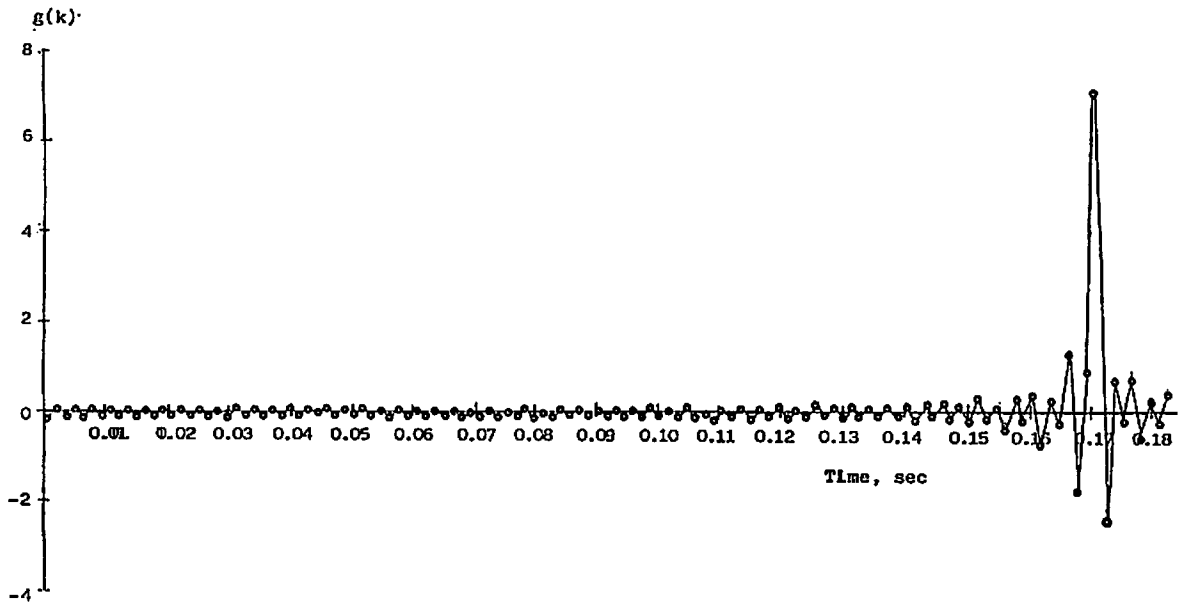


Fig. 5 (a) Simulation result for the impulse response $g(t)$ when no leak existed; $t_\ell = L/C_0$ should be 0.171 sec.

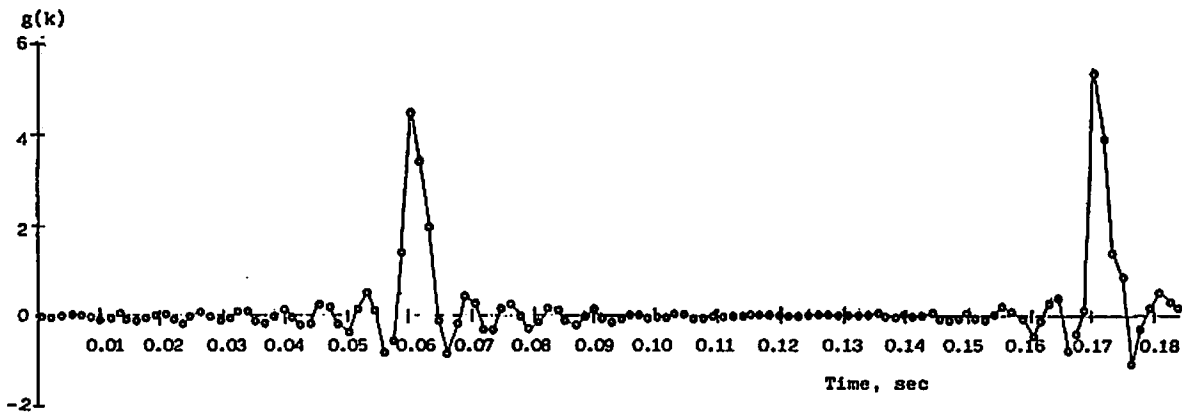


Fig. 5 (d) Simulation result for the impulse response when a leak exists at $l = 39.76\text{m}$; t_ℓ should be 0.0602 sec.

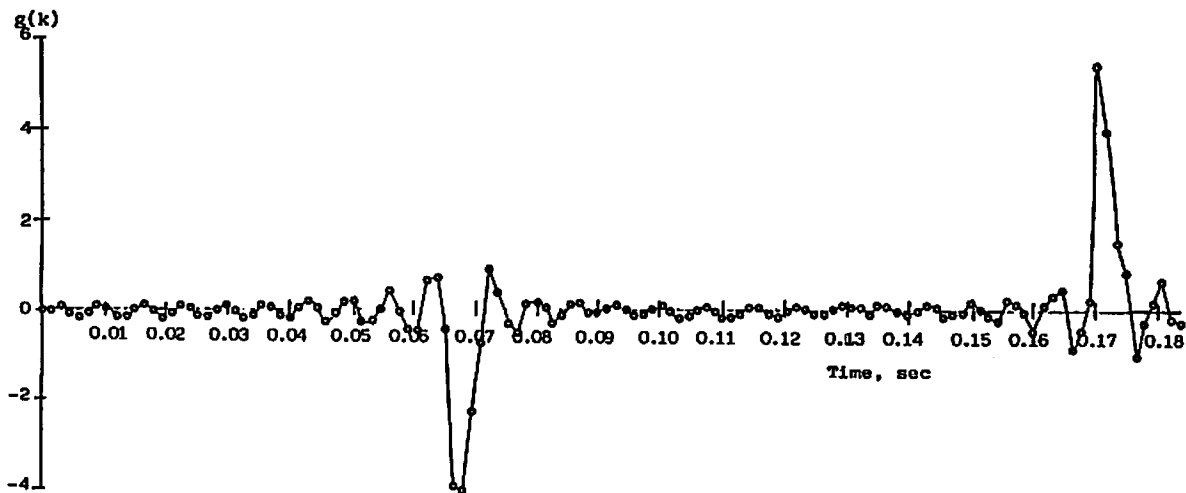


Fig. 5 (c) Simulation result for the impulse response when a leak exists at $l = 17.73\text{m}$; t_ℓ should be 0.0628 sec.

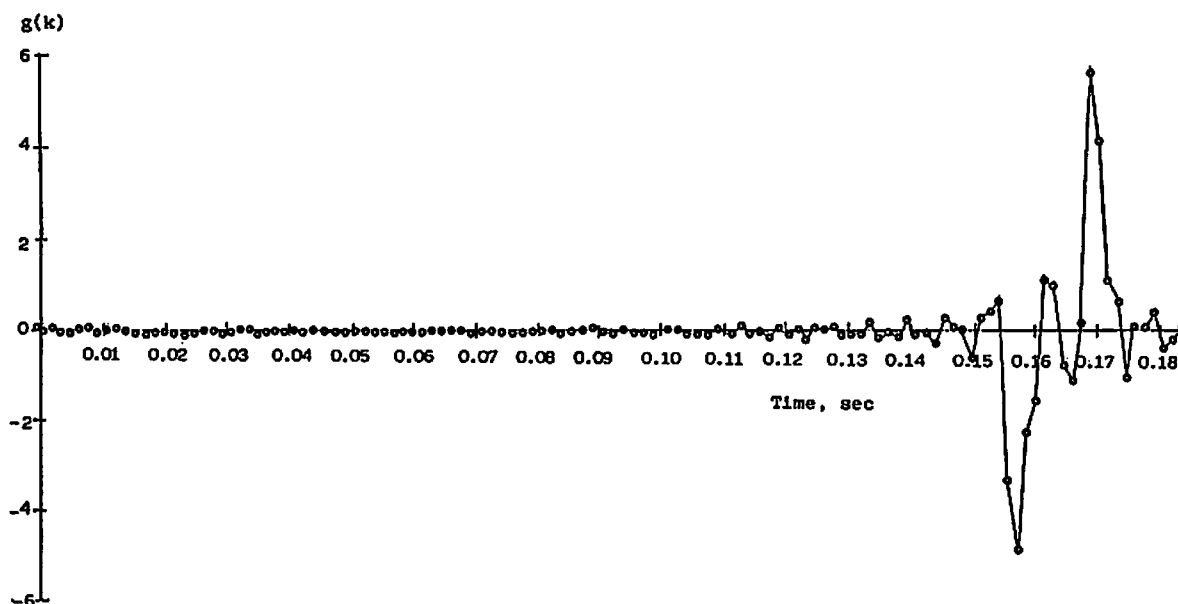


Fig. 5 (b) Simulation result for the impulse response when a leak exists at $\ell = 2.18\text{m}$; t_ℓ should be 0.158 sec.

exists, $g(t)$ must have one positive pulse at $t = 0.171$ sec corresponding to L/C_0 . For the cases in which a leak exists, $g(t)$ must have two pulses. One of them must be positive and must appear at $t = 0.171$ sec corresponded to L/C_0 ; the other must be positive or negative corresponding to a particular leak site as follows:

for $\ell = 2.18\text{m}$, $g(t)$ must have a negative pulse at $t_\ell = 0.158\text{sec}$,

for $\ell = 17.73\text{m}$, $g(t)$ must have a negative pulse at $t_\ell = 0.0678\text{sec}$,

for $\ell = 39.76\text{m}$, $g(t)$ must have a positive pulse at $t_\ell = 0.0602\text{sec}$.

Examination of the simulation results in Fig. 5 indicates the correct positive or negative pulses occurred at the correct times for each leak site.

From Observation (1) in Remarks, the magnitude $\rightarrow 0$ as $\ell \rightarrow L/2$, and the magnitude becomes greater as $\ell \rightarrow 0$ or L . Simulation results demonstrated the similar tendency as Observation (1). The value itself of the magnitude is a relative value and has no particular meaning.

Experimental Results

In this section, we describe the experimental results. Experiments were carried out using the system shown in Fig. 4 (a) and the data obtained by the experiments were processed using the procedure outlined in connection with eq. (6a) ~ eq. (6e). From the result of the leak detection theory summarized in Fig. 3 and the results of simulations in the previous section, the function $g(t)$ or $g(k)$ should have at most two pulses in the period $0 \leq t \leq L/C_0$, and one of them must occur at $t = t_L = L/C_0$. Further from the simulation results, these pulses are big and sharp in comparison with the amplitude of oscillations occurred around times at which pulses were observed. Thus, we observed the estimated impulse

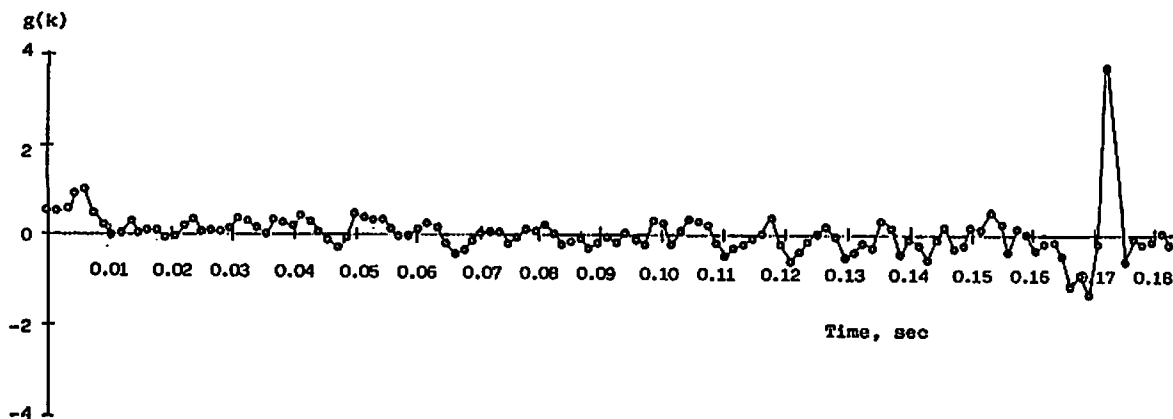


Fig. 6 (a) The impulse response obtained experimentally when no leak existed. Only one pulse at $t = 0.171$ sec should occur according to the Theory.

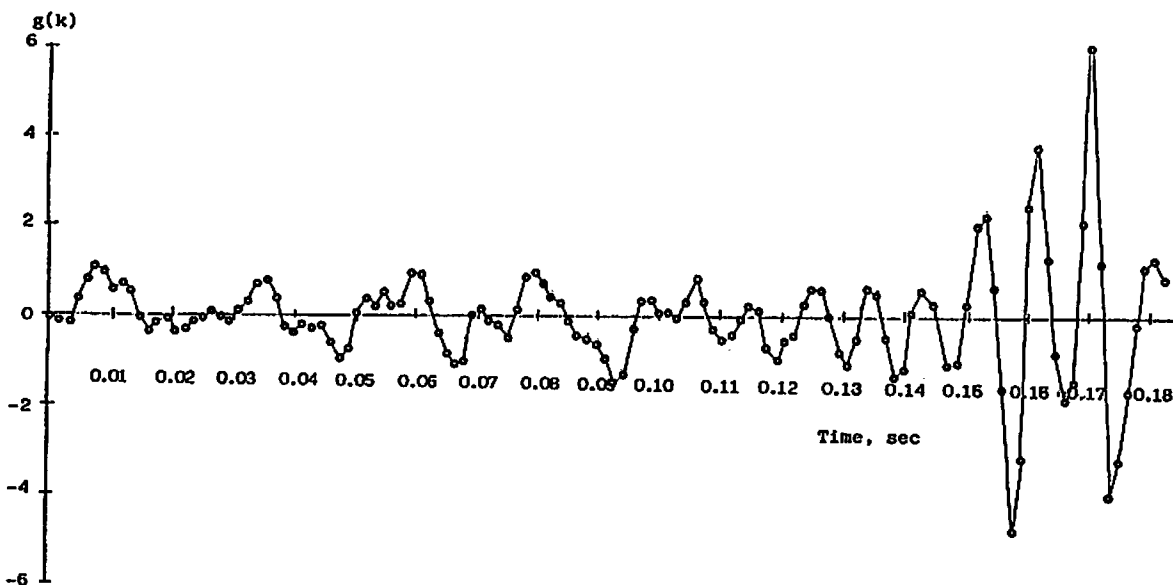


Fig. 6 (b) The impulse response obtained experimentally for the case in which a leak existed at $\ell = 2.18$ m.

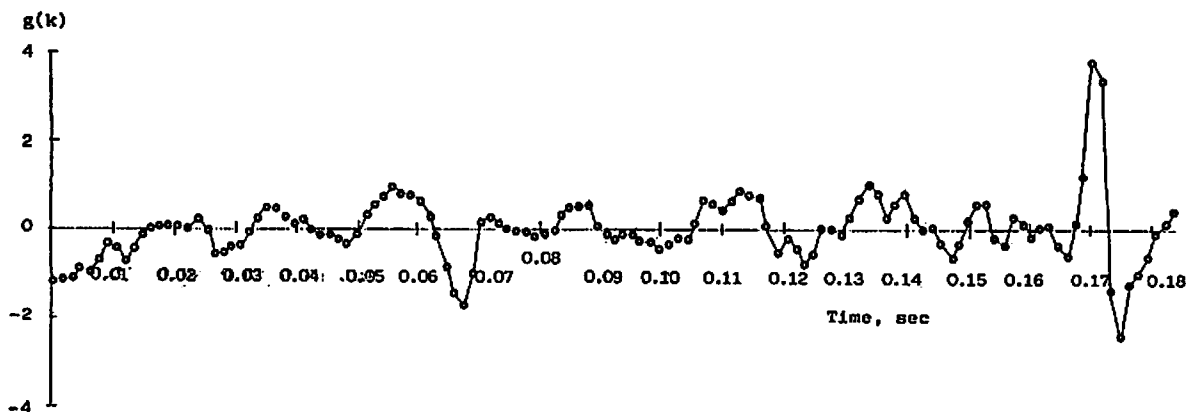


Fig. 6 (c) The impulse response obtained experimentally for the case in which a leak existed at $\ell = 17.7$ m.

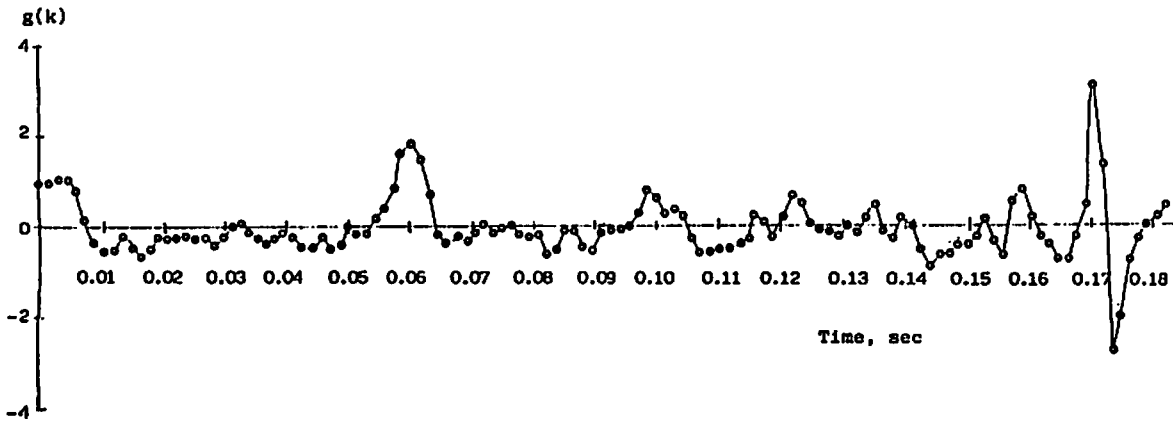


Fig. 6 (d) The impulse response obtained experimentally for the case in which a leak existed at $\ell = 39.76\text{m}$.

response $g(k)$ for the interval $0 \leq t \leq L/C_0 = 0.171\text{sec}$ in a way that where the two biggest pulses occur. Fig. 6 shows the estimated impulse response $g(k)$ for the three different leaks as described above.

Fig. 6 (a) shows the case when no leak exists. As expected, the estimated impulse response $g(k)$ has a sharp pulse at $t_L = 0.171\text{sec}$. No other big pulses were noted for the period $0 \leq t \leq t_L = 0.171\text{sec}$.

Fig. 6 (b)~(d) represents the impulse responses for cases in which the pipeline had a leak. Every impulse response had several pulses. For the interval $0 \leq t \leq 0.171\text{sec}$ the sharp biggest was at or around $t = 0.171\text{sec}$ that corresponded to L/C_0 . The second biggest was that which corresponded to $t = (2\ell - L)/C_0$. Fig. 6 (b) shows that $g(k)$ has the second biggest pulse, one with a negative amplitude at $t = 0.157\text{sec}$. Because the second biggest pulse was negative, from eq. (5a), the leak site ℓ was estimated to be 2.39 m (vs. $\ell = 2.18\text{m}$). Fig. 6 (c) shows that $g(t)$ has the second biggest pulse, one with a negative amplitude, at $t = 0.0662\text{sec}$. Because the second biggest pulse was negative, from eq. (5a), the leak site ℓ was estimated to be 18.0 m (vs. $\ell = 17.73\text{m}$). Finally, Fig. 6 (d) shows that $g(t)$ has the second biggest pulse, one with a positive amplitude, at $t = 0.0603\text{sec}$. Because the second biggest pulse was positive, from eq. (5b), the leak site ℓ was estimated to be 39.8 m (vs. $\ell = 39.76\text{m}$). The numbers of inside of () show the correct distance for leak sites.

The experimental results are quite similar to the simulation results in locating the leak sites. This outcome means that the basic eqs. (1) and eq. (2k) used to develop the leak location theory were appropriate for to the problem, and that the theory is valid. The only the difference between the simulation results and the experimental results was that the experimental results involve noise. In the experiments, the frequency response $G(m)$ was obtained as a stochastic function by using the 17bits M-sequence noise as a test signal, whereas $G(i\omega)$ corresponding to $G(m)$ calculated from eq. (4c) for the simulation is deterministic. Thus, if the noise level ever becomes higher than or significant compared to the

levels of the impulse response, the second biggest pulse may be impossible to distinguish from the other. To reduce the effect of such the failure by chance, we carried out several repeated experiments. From the estimated impulse response $g(k)$ for the interval $0 \leq t \leq L/C_0$, $C_0 = 0.171 \text{ sec}$, we picked up two times at which the first and the second sharp highest pulses (one of them must occur at L/C_0 and the other must occur at $|2\ell - L|/C_0$) occurred and obtained frequency of the occurrences shown as in Fig. 7 (a), (b), (c), and (d). The frequency could discriminate the sharp pulses due to end of the pipeline and/or occurrence of a leak from those by chance.

Figures 7 show the frequency. Fig. 7 (a) demonstrates that occurrences of the pulses are concentrated at one time, namely $t = 0.171 \text{ sec}$ that corresponds to L/C_0 when $L = 58.8 \text{ m}$ and $C_0 = 344 \text{ m/sec}$. The frequency of the other pulses is almost uniformly distributed. In this case of no leak, the magnitude of the second biggest pulse is very small compared to the biggest one. Fig. 7 (b) shows that the pulses are concentrated at only two times, $t = 0.171 \text{ sec}$ (corresponded to L/C_0) and $t_\ell = 0.157 \text{ sec}$ (corresponded to $|2\ell - L|/C_0$, $\ell = 2.18 \text{ m}$). Fig. 7 (c) shows that the pulses are concentrated at only two times, $t = 0.171 \text{ sec}$ and $t \cong 0.0662 \text{ sec}$ (corresponded to $|2\ell - L|/C_0$, $\ell = 17.73 \text{ m}$). Fig. 7 (d) also shows that the pulses are concentrated at $t = 0.171 \text{ sec}$ and $t_\ell = 0.0603 \text{ sec}$ (corresponded to $|2\ell - L|/C_0$, $\ell = 39.76 \text{ m}$)

Thus, even though a single test in some instances may fail to identify a leak site, repeated testing should clearly identify the leak site via frequency counts.

In the experimental set up we used, leaks with cross sectional area of less than $7.07 \times$

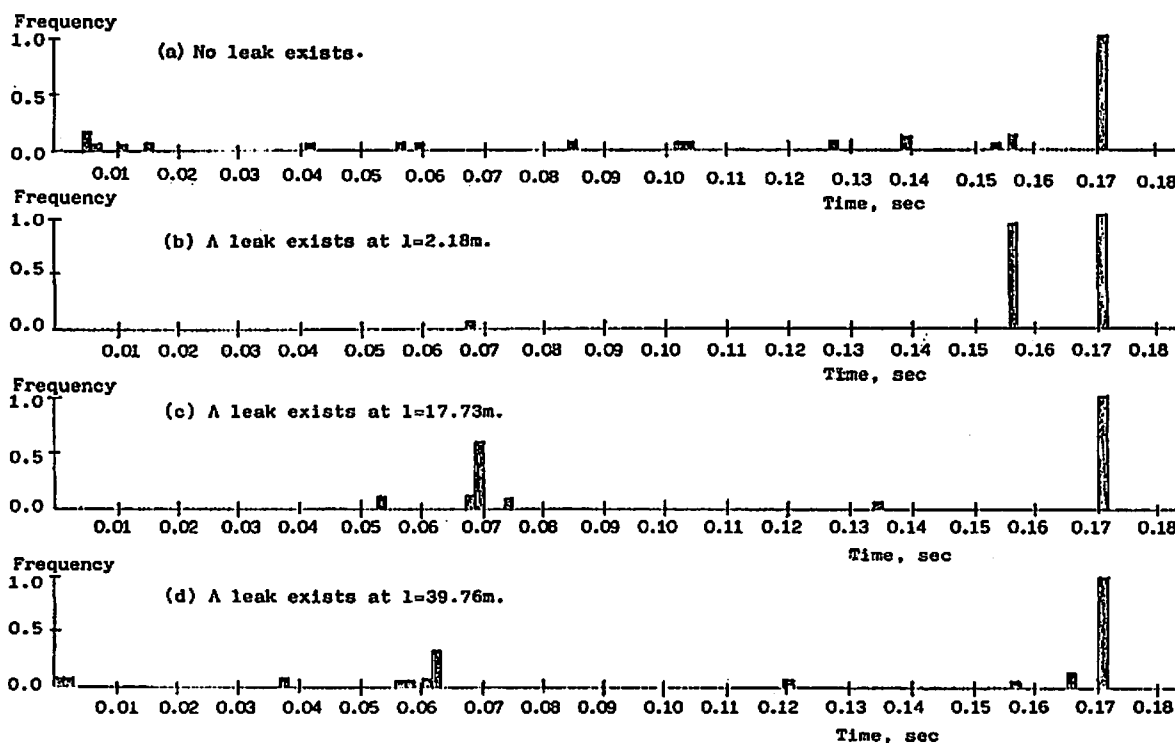


Fig. 7 Frequency of times when the impulses occur

$10^{-6}m^2$ could not be located.

Discussion

The experiments carried out by using the pipeline with 58.8 m length and 22.1cm diameter demonstrated satisfactory leak detection results. We shall consider here what happens when the pipeline or the test zone is long and the cross-sectional area is wide.

General remarks about the effects of cross-sectional area and length of the pipeline were described in **Remarks**. Here, we investigate via calculation, what happens when this method is applied to a realistic pipeline with 20km length and 50cm diameter to locate a leak with diameter of d_ℓ . We assume here, \tilde{k} in eq. (2e) or (4c) is equal to 1.

The coefficients in the last term of eq. (4c) are as follows :

$$\begin{aligned} L &= 20\text{km}, C_o = 344\text{m/sec} \\ A &= \pi(0.5/2)^2 = 0.196\text{m}^2 \\ K &= C_o \frac{3\pi\sqrt{\pi d k}}{16A} = 1.5\pi d_\ell C_o \end{aligned} \quad (8a)$$

The magnitude $K(2\ell-L)/C_o$ given by eq. (7b) and the upper bound of the effective frequency range $5.67\pi C_o/|2\ell-L|$ given by eq. (7c) of the last term in eq. (4c) are functions of the leak site ℓ and these functions are shown in **Fig. 8** (a) and (b).

From eq. (7f), the maximum effective frequency ω_m must satisfy

$$\omega_m > \frac{56.7\pi C_o}{L} = 3.06 \text{ rad/sec (0.487Hz)} \quad (8b)$$

Suppose

$$\omega_m = 5.4 \text{ rad/sec (=0.859Hz)} \quad (8c)$$

Then from eq. (7f) and eq. (7g), the sampling interval and the minimum resolution of identification of the leak site becomes

$$\tau = \frac{\pi}{\omega_m} = 0.924 \text{ sec} \quad (8d)$$

$$\Delta x = \frac{\pi C_o}{2\omega_m} = 100 \text{ m} \quad (8e)$$

Further from eq. (7i), we can choose N as follow :

$$\frac{\omega_m L}{\pi C_o} = 100 \ll N = 2048 \quad (8f)$$

From eq. (7h)

$$\Delta\omega = 3.32 \times 10^{-3} \text{ rad/sec (=5.28} \times 10^{-4} \text{ Hz)} \quad (8g)$$

From **Fig. 8** (a), if the diameter of a leak is 1 cm (area of the cross-section = $7.86 \times 10^{-5}m^2$), the magnitude of the last term of eq. (4c) is greater than 1 (the magnitude of the first term) for the leak $0 \text{ km} \leq \ell \leq 10\text{km} - 33.3\text{m}$ and $10\text{km} + 33.3\text{m} \leq \ell \leq 20\text{km}$ which covers 99.7% of the length of the test zone.

Eq. (7e) or eq. (8b) shows only the lowest bound of the maximum effective frequency

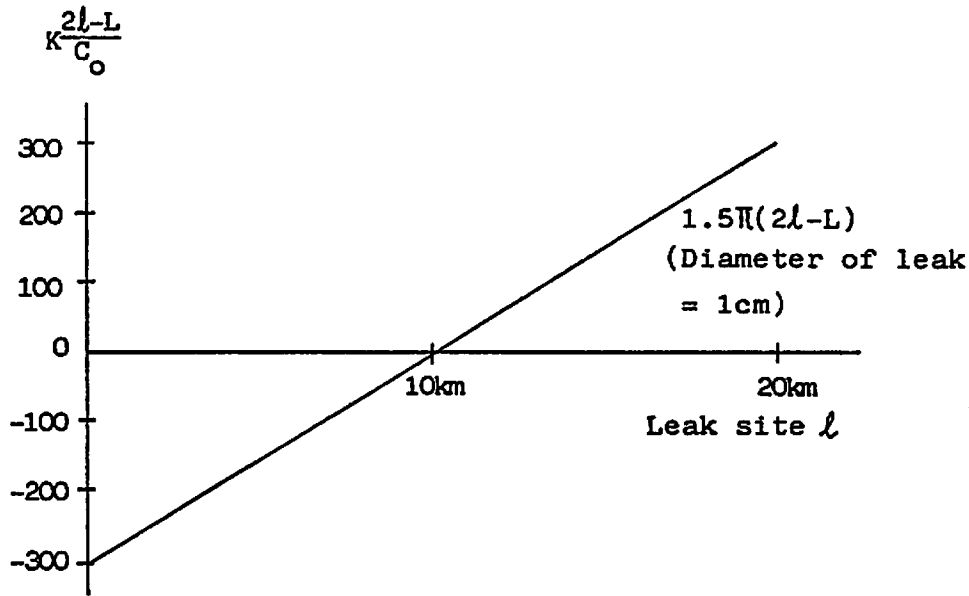


Fig. 8 (a) Magnitude of $\frac{K}{\omega} \sin \frac{\omega(2-L)}{C_0}$, the last term of eq (4c)

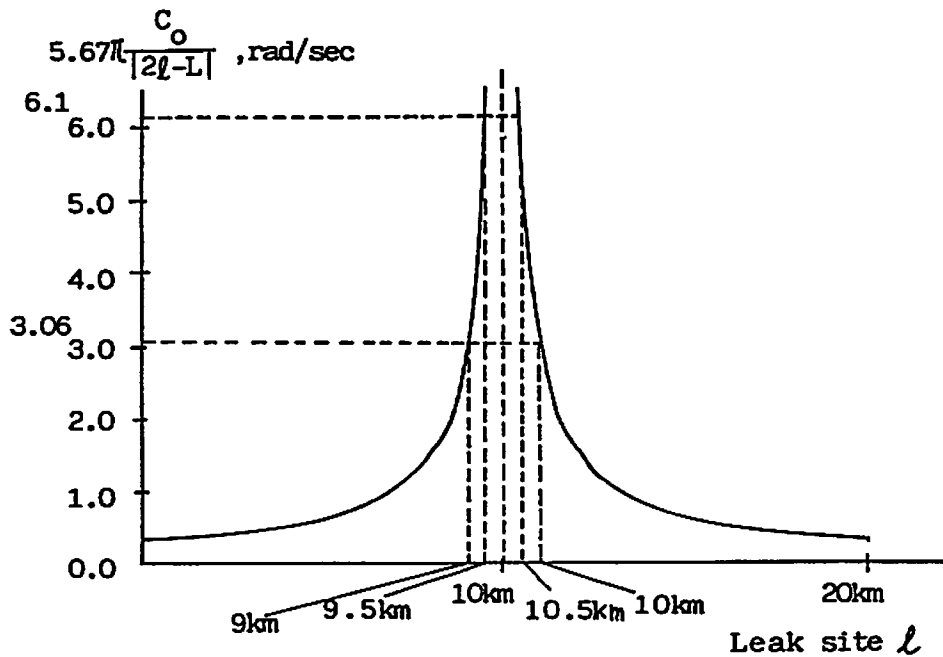


Fig. 8 (b) Maximum frequency range vs. leak site l

ω_m . Thus, so far as the limitation (7e) or (8b) concerned, we can select any higher frequency as ω_m by employing a noise generator and acoustic signal detectors with broader frequency band width. From eq. (7g) or eq. (8e), the choice of broader ω_m yields higher resolution of identifiability of the leak site. However, high frequency noises that are generated enough near to be caught by one of the detectors but too high (higher than $56.7\pi C_0/L$ rad/sec in eq. (8b)) to propagate to the other acoustic detector will disturb the estimation of the accurate transfer function (4c). There are many causes of local generation of noises, i. e., (1) high frequency part of external noise on the pipeline, (2) pump noise, (3)

compressor noise, (4) noise that might come from the pipe vibration due to the leak itself (in the 500–800Hz range) and (5) noise due to the impact of gas on the soil surrounding the pipe (20–250Hz range). Thus, in determining the frequency ω_m , we must take into account the local high frequency noise that should be cut off. The choice of the frequency $\omega_m=5.4\text{rad/sec}$ ($=0.859\text{Hz}$) as eq. (8c) can cut off such the local noise undesired. The low frequency part ($0\leq\omega\leq 5.4\text{ rad/sec}$) of the noise occurred near the input constriction can be utilized as the test signal.

There are many ways to enhance the pulse corresponded to the leak site in eq. (4e) or in Figures 6 from noises. One of them is to let $\Delta\omega$ defined by (7h) and given by (8g) for 20km pipeline be small by increasing number of data points N as mentioned in **Remarks**. Stochastic approaches for repeated testings such as we applied in obtaining the results shown in **Fig. 6** or just averaging of the final results $g(k)$ can enhance the pulse. Further, since we have the theoretical model (4c) with the known important coefficients L , C_0 and A for the estimated transfer function (6a), we can also formulate this leak location problem to estimate the unknown ℓ to fit the estimated transfer function to eq. (4c).

In the case when flow occurs in the pipeline, the leak detection and location theory is required modifications. The theory should be developed based on eq. (4a). The presumable leak detection and location procedure is as follows:

- (1) Multiply $\exp(-i\omega L/v')$ to the estimated transfer function corresponding to eq. (4a) to eliminate the term $\exp(i\omega L/v')$. The term can be calculated because L is known and v' is calculated by the values C_0 and v .
- (2) Apply the Fourier inverse transform to the term $\exp(-i\omega L/v') \times (4a)$ estimated.
- (3) The result of (2) yields a sharp positive pulse at L/C' and a sharp positive or negative pulse at $|2\ell-L|/C'$. The parameter C' is calculated by using eq. (2i).
- (4) By the results of (3), we can identify the leak location ℓ as we did in the case when $v\cong 0$.

This procedure is basically same with the procedure outlined in eq. (6a) to eq. (6e) if we let $v=0$.

Nomenclature

A	cross sectional area of the pipeline
a	arbitrary positive constant
$b(x,t)$	sound volume velocity propating backward
c	arbitrary positive constant
C_0	velocity of sound
C_b	total velocity of sound propagating backward
C_f	total velocity of sound propagating forward
C'	sound velocity when flow occurs in the pipeline

DFT	discrete Fourier transform
d	cross sectional area of the leak
d_ℓ	diameter of a circular leak
$e_{i,j}$	(i,j) element of the transfer matrix
$F(\)$	transfer matrix that characterizes the acoustic propagation in a pipeline
$f(x,t)$	sound volume velocity propagating forward
$f_{i,j}$	(i,j) element of the effective transfer matrix
$G(m)$	transfer function estimated
$G(i\omega)$	transfer function, the Fourier transform of $g(t)$
$g(k)$	impulse response estimated
$g(t)$	impulse response function
$g_i(t)$	i -th term of the function $g(t)$
IDFT	inverse discrete Fourier transform
i	imaginary unit
K	constant determined by the cross-sectional area of a leak
k	discrete time
\tilde{k}	compensating coefficient of radiation impedance
L	length of the test zone of the pipeline
ℓ	site of the leak measured from the input site
ℓ^-	input site of ℓ
ℓ^+	output site of ℓ
m	discrete frequency
N	number of data sampled
$P(x,i\omega)$	Fourier transform of the sound pressure
$p(x,t)$	sound pressure
$p_i(t)$	sound pressure at the input site of the test zone
$p_o(t)$	sound pressure at the output site of the test zone
Re	real part of complex numbers
r	ratio (cross-sectional area of the constriction/cross-sectional area of the pipeline)
t	time
t_ℓ	time when the pulse due to a leak occurs
t_L	time when the pulse occurs due to the constriction at the end of the test zone
$U(x,i\omega)$	Fourier transform of the sound volume velocity
$u(x,t)$	sound volume velocity
v	velocity of flow
v'	velocity of flow influenced by the sound velocity in the pipeline
x	distance from the input site of the test zone
Z_ℓ	radiational acoustic impedance of the leak
z	arbitrary variable
<i>Greek</i>	
∂	partial differentiation
π	$=3.1415926$
ρ	density of gas
τ	sampling interval
ω	angular frequency
ω_i	lowest angular frequency of the signal considered
ω_h	highest angular frequency of the signal considered
ω_m	effective maximum angular frequency
$\Delta\omega$	step size of angular frequency for discrete spectrum function

Symbols

| 1 | absolute value

References

- Cole, E. S., "Methods of Leak Detection: An Overview", *J. Amer. Water Works Assn.*, Feb., P. 73., 1979.
- Dallavalle, F., G. Possa, and F. Tonlini, "Early Leak Detection in Power Plant Feedwater Preheaters by Means of Acoustic Surveillance," *Symp. On Line Surveillance and Monitoring of Process Plant*, City Univ. London, sept. 1977, p. 241.-248.
- Decker, H. W., "Pipeline Leak Detection Using Nitrous Oxide Method," *Pap. Summ. ASNT. Conf. (U. S.A.)*, pp. 358-359, 1978.
- Goldberg, D. E., "Transient Leak Detection", *Conf. Prp. Int. Pipeline Technol. Conf. (U.S.A.) 7th*, pp. 117-188, 1979.
- Heim, P. M., "Leakage Detection on Buried Pipelines," *Conf. Pap. Int. Pipeline Technol. Conf (U.S.A.) 7th*, pp. 169-176, 1979.
- Huebler, J. E., N. C. Saha, and J. M. Craig, *Identification of Leaks-Internal Acoustic Techiques*, Report GRI-8010142, Institute Gas Technology, Chicago, Illinois, Aug., 1982.
- Huber, D. W., "Real-time Transieut Model for Batch Tracking, Line Balance and Leak Detectien," *J. Con. Pet. Technol*, vol. 20, no. 3, pp. 46-52, 1981.
- Kreiss, M., "Schnelle Erkennung von Leakagen an Rohrfernleitungen," *Erdöl unt Kohl-Erdgas-Petrochemie mit Brennstoff-Chemie*, vol. 25, no. 7, pp. 402-409, 1972.
- Lindsey, T. P. and Vanelli, J. C., "Real-Time Flow Modeling," *Rec. Conf. Pap. Annu. Pet. Chem. Ind. Conf. (U.S.A.) 28 th*, pp. 189-192, 1981.
- Parker, J. G. and Jette, A. N., "Surface Displacements Accompanying the Propagation of Acoustic Waves an Underground Pipe," *J. Sound and Vibr.* vol. 69, 1980.
- Ohizumi, J. etal, "Speech Synthesis," *Lattice Publishing Company*, Tokyo, 1968.
- Phillips, R. D. and Crider, C. W., "Microcomputers Used in Metering and Leak Detection System for Liquid Petroleum Products Pipeline," *IEEE trans. Ind. Appl.* vol IA-12, no. 6, pp. 341-348, July/August, 1976.
- Riemsdijk, A. J. and Bosserlaar, H., "On-Stream Detection of Small Leaks in Criude Oil Pipeline," *Proc. of 7 th World Petroleum Congress*, 1960.
- Schmidt, G. K. and Lappus, G., "Dynamical Observers for State Reconstrunction and Leak Detection in Natural Gas Pipeline Systems," *Proc. Jt. Autom. Control. Conf. (U.S.A.)*, 1982(2), SP 6. E1-E2, 1980.
- Seiders, E. J., "Hydraulic Gradient Eyes In Leak Location," *Oil. Gas J. (U.S.A.)*, vol. 77, no. 47, pp. 112-125, 1979.
- Siebert, H., *Evaluation of Different Methods for Pipeline Leaking Monitoring*, Document KFK-PDV-206, Kernforschungsanlage Juelich G.m.b.H. West Germany, Sept., 1981.
- Siebert, H. and Isermann, R., "A Method for The Detection and Localization of Small Leaks in Gas Pipelines," *Automation for Safety in Shipping and Offshore Petroleum Operations* pp. 355-360, 1980.
- Stewart, T. L., " On-line Computer Detects Leaks on Ozark Line," *Oil. Gas. J. (U.S.A.)*, vol. 78, no. 39, pp. 108-111, 1980.
- Sugaya, S., "Present Situation of Leak Detection Techniques for Pipelines," *J. SICE*, (Japan) vol. 18, no. 5, pp. 425-430, 1979.
- Watanabe, K. and Sogo, S., "A Detecton Method of Leak Locations in a Gas Transport Pipeline by Use of Its Acoustic Characteristics," *Trans. SICE*, (Japan) vol. 16, no. 6., pp. 885-890, Dec. 1980.
- Watanabe, K., "On Locating a Leak of Gas Transport Pipeline by Acoustic Method," *The J. of Fluid Cotrol*, vol. 14, no. 1, pp. 39-55, March, 1982.